1556 *Macromolecules* **2010**, *43*, 1556–1563
DOI: 10.1021/ma9019416

Macromolecules
ARTICLE

Nonuniformity in Cross-Linked Natural Rubber as Revealed by Contrast-Variation Small-Angle Neutron Scattering

Takuya Suzuki, Noboru Osaka, Hitoshi Endo, and Mitsuhiro Shibayama*

Institute for Solid State Physics, The University of Tokyo, Kashiwa, Chiba 277-8581, Japan

Yuko Ikeda,* Hanako Asai, Norihito Higashitani, and Yota Kokubo

Graduate School of Science and Technology, Kyoto Institute of Technology, Matsugasaki, Sakyo, Kyoto 606-8585, Japan

Shinzo Kohjiya

Department of Chemistry, Faculty of Science, Mahidol University, Salaya Campus Phuthamonthon, Nakorn Pathom 73170, Thailand

Received September 1, 2009; Revised Manuscript Received November 8, 2009

ABSTRACT: The microscopic structures of cross-linked natural rubber (NR) were investigated by means of contrast-variation small-angle neutron scattering (CV-SANS) coupled with "visualization-by-swelling method" as a function of dicumyl peroxide (DCP; cross-linker) content, where the various types of inhomogeneities in the rubber were visualized by swelling with deuterated solvent. Detailed analyses of the partial scattering functions of each component confirm the existence of network inhomogeneities due to cluster-like structures of polyisoprene chains as well as larger inhomogeneities of protein aggregates. The observed partial scattering functions of polyisoprene with different DCP contents clearly exhibited that (1) the network inhomogeneities were strongly suppressed by DCP addition and (2) the structure of protein aggregates was not significantly influenced by the introduction of the peroxide cross-linking. These nanoscopic structural aspects with respect to the content of cross-linker provide better understanding of the elastic properties of NR.

1. Introduction

Natural rubber (NR) is one of the most important materials, which has been widely used in industry as well as in our daily life, e.g., pneumatic tires, tubes, films like surgical gloves, rubber bands, etc. The versatility of NR is originated by its toughness based on the outstanding tensile properties and excellent crack growth resistance.[1−8] NR is obtained from *Hevea brasiliensis*[9,10] and consists of ca. 94% polyisoprene, and about 2.2% of proteins and 3.4% of lipids are known to be other contaminants.[9−11] Such minor components, i.e., proteins, phospholipids, fatty acids, carbohydrates, and inorganic substances, have been believed to provide these marvelous properties of NR by lots of rubber technologists. Tanaka presumed by ^{13}C and ^{1}H NMR spectroscopy that both the aggregates of proteins and phospholipids act as cross-linking points, where α-terminal groups of main chain of NR interact with phospholipids via ionic linkage and ω-terminal groups do with proteins through hydrogen bonds.[12,13] Kohjiya et al. studied an effect of stearic acid, which is one of the fatty acid, on strain-induced crystallization (SIC).[14] They clarified that stearic acid is not necessary for SIC, while it has been presumed to act as a nucleating agent for temperature-induced crystallization. In spite of these works on the roles of nonrubber components such as the phospholipids and proteins in NR, the question has been still mysterious mainly because even deproteinized NR (DPNR) is known to show excellent properties as crude NR.[15,16]

*To whom correspondence should be addressed. E-mail: (M.S.) sibayama@issp.u-tokyo.ac.jp; (Y.I.)yuko@kit.ac.jp.

Cross-linking is the most important process in the rubber manufacturing process. There are typically two types of cross-linking, i.e., sulfur and peroxide ones.[8] Sulfur cross-linking (vulcanization) has been known to be the complicated reactions between rubber, elemental sulfur, and other cross-linking reagents, in spite of its long history since 1839.[9,8,10,17,18] Hagen et al. studied the viscoelastic properties by mechanical spectroscopy and disclosed that sulfur-cross-linked NR has higher glass transition temperature than peroxide cross-linked one.[19] Ikeda et al. recently studied the local structures of sulfur cross-linked polyisoprene (PI) rubber by small-angle neutron scattering (SANS) and wide-angle X-ray diffraction (WAXD), and elucidated that the size of network domains increased by the introduction of sulfur cross-linking due to the adsorption of sulfur onto ZnO particles, which are activators or auxiliary accelerators for cross-linking.[20] In contrast, peroxide cross-linking is a reaction acting on polyisoprene chains via dehydrogenation, which is accompanied by the production of free radicals, giving rise to high thermal resistance.[8,21] Since most of the previous studies on NR deal with sulfur cross-linked system, it should be a crucial matter to study the local structures of proteins and polyisoprene chains in NR from the viewpoint of the peroxide cross-linking effect.

Small-angle neutron scattering (SANS) has been one of the most powerful tools for structural characterization of polymeric systems. Moreover, SANS technique can be highly useful even for NR because it makes invisible network structure "visible" by immersing the polymer in deuterated solvent and succeeding

 Published on Web 01/07/2010

Table 1. Recipe and Properties of the Rubber Sample

	NR0	NR10	NR20
rubber	100	100	100
DCP[a] (phr[b])	0	1.0	2.0
Q		5.79	4.82
PI (vol %)	15.7[c]	15.9[d]	18.4[d]

[a] Dicumyl peroxide. [b] Part per one hundred rubber by weight. [c] Volume fraction of polyisoprene calculated from the sample preparation condition. [d] Volume fraction of polyisoprene calculated from the swelling degree.

swell of polymer chains. We call this method "visualization-by-swelling method". Karino et al. carried out SANS study for NR in deuterated toluene (D-toluene) as a solvent and showed that there exist large inhomogeneities originating from protein aggregates, in addition to the blob scattering visualized by this method.[16] They also studied NR samples with different peroxide-cross-link densities. However, the cross-linking density dependence of the polyisoprene network structure was left unsolved. This was partially due to the fact that the experimental detection of the cross-linking effect was disturbed by strong scattering from protein aggregates. Contrast-variation SANS (CV-SANS) technique with hydrogen−deuterium exchange can circumvent this problem and allow one to study the nanoscopic structure of target materials.[22,23] One of the advantages of the CV-SANS method is the usability in multicomponent systems provided that each scattering density of the components is precisely determined. Therefore, an application of CV-SANS to NR can be a challenging work for the understanding of the peroxide cross-linking dependence if we carefully treat the inherent complexity of the composition in NR. As far as we know, there have been no reports that studied the local structure of NR for peroxide cross-linked system by CV-SANS. In this study, we have studied the structural inhomogeneities and the local structure of the protein and polyisoprene of peroxide-cross-linked NR by CV-SANS coupled with visualization-by-swelling method. For comparison, DPNR and noncross-linked NR were also studied.

2. Experimental Section

2.1. Rubber Samples. In order to clarify the effect of cross-linking, raw rubber, i.e., NR (RSS No. 1 from Indonesia), was subjected to two-roll milling without any reagents and heat-pressing at 155 °C for 30 min in a mold. Thus, obtained reference sample is abbreviated as NR0. DPNR (DPNR 6110, Sumitomo Rubber Co.) were used as received. The details were given elsewhere.[16]

2.2. Cross-Linked Rubber Samples. Peroxide cross-linked NR samples were prepared as follows: NR was mixed with dicumyl peroxide (DCP) on a two-roll mill. The mix was cured under a heat-pressing at 155 °C for 30 min in a mold to give cross-linked rubber sheet of 1 mm thickness. The sample codes of the cross-linked NRs with DCP contents of 1.0 phr or 2.0 phr are defined as NR10 and NR20, respectively. The ingredients of NR0, NR10 and NR20 are summarized in Table 1 together with the degree of swelling, Q, of the cross-linked samples, and the volume fraction of polyisoprene. Q was calculated using the equation $Q = V_s/V_0$, where V_0 and V_s are the volumes before and after swelling in toluene, respectively. The details of the swelling degree measurement were given elsewhere.[16] The all samples were swollen in toluene, and then measured by SANS. Planar quartz cells of 1 or 2 mm thickness (depending on the sample transmission) × 10 mm width × 40 mm height were used for SANS measurements.

2.3. CV-SANS. SANS experiments were performed at the SANS-U instrument owned by Institute for Solid State Physics, The University of Tokyo located at JRR-3 research reactor of Japan Atomic Energy Agency in Tokai, Japan.[24] The neutron wavelength was 7.0 Å with ca. 10% fwhm. The wavelength distribution of SANS-U is about 13%. We examined the effect of polychromacity for polystyrene latex with polystyrene spheres of ca. 500 Å in diameter.[25] The results indicated polychromacity was insignificant for systems unless the polydispersity is small, e.g., 10% or less. Since the polydispersity of the scattering objects in this work was much larger than that of the polystyrene latex, we assumed that polychromacity effect was negligible. The sample-to-detector distance was chosen to be 2 and 8 m, and the magnitude of the corresponding scattering vector, q, was from 0.005 to 0.15 $Å^{-1}$. In order to perform CV-SANS experiment, the necessary corrections were made, such as air scattering, cell scattering, and incoherent background subtraction.[26] After these corrections, the scattering intensity was normalized to the absolute intensity with a polyethylene secondary standard sample. The temperature of the samples was regulated to be 25 °C with the precision of ±0.1 °C.

Table 2. Mass Density and SLD of Each Component in NR Samples

	mass density (g/cm^3)	ρ ($\times 10^{10}$ cm^{-2})
polyisoprene	0.93	0.27[a]
protein		
D-toluene	0.943	5.66[a]
toluene	0.867	0.94[a]
phospholipid		0.32[b]

[a] Calculated from the chemical structures and mass densities. [b] The typical average SLD of phospholipids.[27,28]

For CV-SANS, we assumed the swollen NR as the three-component system with polyisoprene, protein, and solvent (toluene). This is due to the fact that among the nonrubber components, protein gives rise to strong scattering due to its aggregated structure.[16] The scattering length densities (SLD), ρ, of each component in natural rubber are given in Table 2. It should be noted that the typical average SLD of phospholipids is 0.32×10^{10} cm^{-2} and is almost the same as that of polyisoprene ($=0.27 \times 10^{10}$ cm^{-2}).[27−29,20] Moreover, the volume fraction of phospholipids is much smaller than that of polyisoprene. Therefore, the contribution of phospholipids to the total scattering intensities can be included into that of polyisoprene. We hereafter represent polyisoprene as implicitly including phospholipids.

In the case of ternary system with protein, polyisoprene, and toluene as solvent, the scattering intensity can be described as[22,23,30]

$$I(q) = (\rho_P - \rho_S)^2 S_{PP}(q) + 2(\rho_P - \rho_S)(\rho_I - \rho_S) S_{PI}(q) + (\rho_I - \rho_S)^2 S_{II}(q) \quad (1)$$

where $S_{jk}(q)$ is a partial scattering function, and ρ_j represents the scattering length densities (with j or k = P, I, and S for protein, polyisoprene, and solvent (toluene), respectively). The aim of the contrast variation experiments is decomposition of the observed scattering intensity into the partial scattering functions. Contrast variation experiments can be realized by playing with H/D replacement of the solvent. Regarding ternary systems, partial scattering functions are uniquely determined with three different scattering contrasts. With more than three different scattering contrasts in ternary systems, the overdetermined scattering intensities can be decomposed into three partial scattering functions via singular value decomposition. The details of the contrast variation experiments can be found elsewhere.[31]

In order to vary the scattering contrast in this study, a series of samples with different SLD of solvent were prepared. Each SLD was calculated on the basis of the chemical structures and mass densities. The mass densities of the components are 0.93 g/cm^3 for polyisoprene, 0.867 g/cm^3 for toluene, and 0.943 g/cm^3 for D-toluene. We changed SLD of the solvent, $\rho_{toluene}$, by varying the volume fraction of deuterated toluene, $\phi_{D\text{-}toluene}$. Here,

Table 3. SLD of Amino Acid and the Amino Acid Content of the Protein in NR

amino acid	chemical composition	b (10^{-12} cm)$^{2\,a}$	v (Å^3)^b	ρ_A (10^{10} cm^{-2})^c	N^d
glycine	C_2NOH_3	1.728	66.4	2.60	32
alanine	C_2NOH_5	1.645	91.5	1.80	27
valine	C_5NOH_2	1.479	141.7	1.04	23
leucine	C_6NOH_{33}	1.396	167.9	0.83	30
isoleucine	C_6NOH_{33}	1.396	168.8	0.83	16
phenylalanine	C_2NOH_2	4.139	203.4	2.03	13
tryosine	$C_2NO_2H_2$	4.719	203.6	2.32	15
tryptophan	$C_{33}N_2OH_{30}$	6.035	237.6	2.54	9
aspartic acid	$C_4NO_3H_4$	3.845	113.6	3.38	10
glutamic acid	$C_5NO_3H_6$	3.762	140.6	2.68	13
serine	$C_3NO_2H_5$	2.225	99.1	2.24	41
threonine	$C_4NO_2H_7$	2.142	122.1	1.75	17
asparagine	$C_4N_2O_2H_6$	3.456	135.2	2.56	14
glutamine	$C_5N_2O_2H_8$	3.373	161.1	2.09	23
lysine	$C_6N_2OH_B$	1.586	176.2	0.90	22
arginine	$C_6N_4OH_B$	3.466	180.8	1.92	20
histidine	$C_6N_3OH_{6,5}$	4.959	167.3	2.96	
methionine	C_5NOSH_2	1.764	170.8	1.03	1
cysteine	C_3NOSH_5	1.930	105.6	1.83	
proline	C_5NOH_7	2.227	129.3	1.72	15

[a] Scattering length.[32] [b] Specific volume.[32] [c] Scattering length density calculated on the assumption of the sharp surface. [d] Relative number of molecules of the denatured protein in NR.[33]

$\rho_{toluene}$ is given by

$$\rho_{toluene}(\phi_{D\text{-}toluene}) = 5.66 \times \phi_{D\text{-}toluene} + 0.94 \times (1 - \phi_{D\text{-}toluene})[10^{10}\ cm^{-2}] \quad (2)$$

On the other hand, SLD of a protein depends on the amino acid composition. Therefore, the detailed discussion of the average SLD of protein, ρ_P, is given in the next section.

3. Results and Discussion

3.1. Estimation of the Scattering Length Density of the Protein in NR, ρ_P. In order to perform CV-SANS, precise determination of the scattering length densities (SLD) for each component is one of the necessary demands. In the case that proteins are dissolved in aqueous solution, it is known that the protons contained in amino groups and hydroxyl groups can be exchanged for the protons in the water solution. In particular, this effect is not negligible when heavy water is used as the solvent.[32] In this study, however, since toluene was used as the solvent in order to swell NR, the above-mentioned exchange effect does not occur.

For the calculation of SLD of the protein in the system, ρ_p, the content of amino acids must be known. Table 3 is a list of amino acids in the proteins of NR, which gives the values of SLD for each amino acid, ρ_A. We adopted the amino acid composition in NR and their specific volume, v, which were taken from refs 32 and33, respectively, which are the values in water. By applying these quantities, ρ_p can be calculated on the assumption of the sharp surface as[33]

$$\rho_P = \frac{\sum_i \rho_{Ai} v_i N_i}{\sum_i v_i N_i} \quad (3)$$

where the subscript i denotes the ith amino acid. The obtained value was 1.8×10^{10} cm^{-2}, which is the same as the typical SLD of the protein in water.[32,34] We hereafter apply SLD of proteins as $\rho_P = 1.8 \times 10^{10}$ cm^{-2}.

Figure 1 shows SLD, ρ, of each component as a function of the volume fraction of deuterated toluene in the solvent, $\phi_{D\text{-}toluene}$. $\rho_{toluene}$ varies linearly with $\phi_{D\text{-}toluene}$ according to eq 2. It should be noted that contrast matching between polyisoprene and the solvent cannot be realized in this system because of $\rho_I < \rho_S$. On the other hand, the theoretical matching point of the protein was determined to be

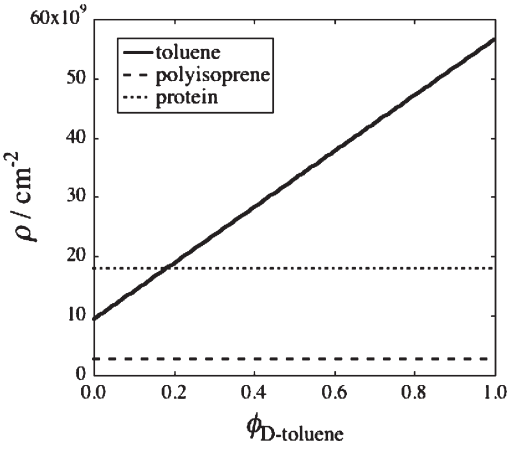

Figure 1. Variation of the scattering length density ρ of each component as a function of $\phi_{D\text{-}toluene}$.

$\phi_{D\text{-}toluene} = 0.18$, where $\rho_{toluene}$ is matched with ρ_P. We can deduce that the scattering from both polyisoprene and protein should be extremely weak at $\phi_{D\text{-}toluene} = 0$ due to the low scattering contrast while the efficiently large scattering signal is expected to be obtained at $\phi_{D\text{-}toluene} = 1.0$.

3.2. Comparison between DPNR and NR0. Prior to the CV-SANS results, let us compare the scattering signals between DPNR and NR0. Figure 2 exhibits the absolute scattering intensities before the subtraction of incoherent background, $I(q)$'s, at (a) $\phi_{D\text{-}toluene} = 0$ and (b) $\phi_{D\text{-}toluene} = 1.00$ for DPNR and NR0. The polymer concentrations were 16.7 and 16.8 vol % and the sample thicknesses were t = 1 mm, and 2 mm, respectively for the cases of $\phi_{D\text{-}toluene} = 0$ and $\phi_{D\text{-}toluene} = 1.00$. The scattering profiles in the low q region are obviously different depending on the presence (NR0) or absence (DPNR) of the protein. In the case of $\phi_{D\text{-}toluene} = 0$ exhibited in Figure 2a, the scattering profile of DPNR is flat because it includes no protein and the scattering contrast between the polyisoprene and solvent is too small to be detected. For NR0, the upturn in the low q region appeared, which originates from the protein aggregates, as discussed by Karino el al.[16]

In the case of $\phi_{D\text{-}toluene} = 1.00$ depicted in Figure 2b, $I(q)$'s are much larger than those of Figure 2a due to the enhancement of scattering contrast between the solvent and the other

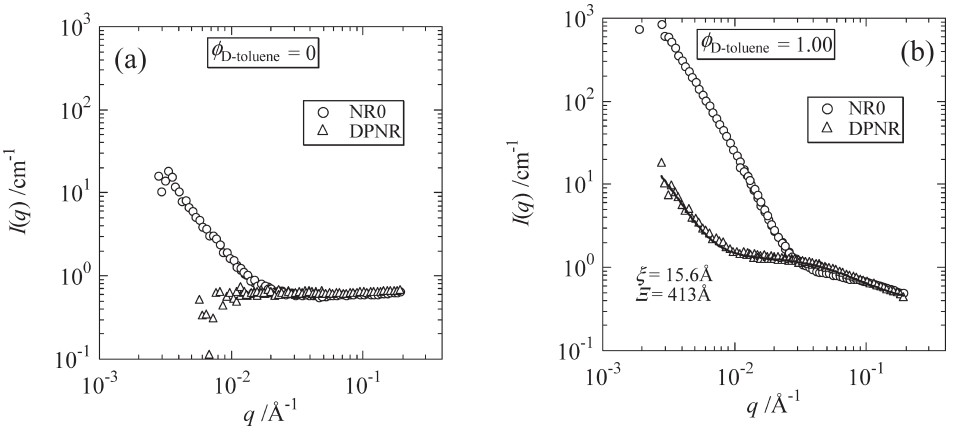

Figure 2. Absolute scattering intensities before the subtraction of incoherent background, $I(q)$'s, at (a) $\phi_{\text{D-toluene}} = 0$ and (b) $\phi_{\text{D-toluene}} = 1.00$ for DPNR and NR0. The polymer concentrations were 16.7 and 16.8 vol % and the sample thicknesses were $t = 1$ mm, and 2 mm, respectively for the cases of a and b. The solid line in part b denotes the result of curve-fit with eq 4.

solutes. In addition, the shoulder was observed in the high q region. This was driven by the scattering of the partial chains of polyisoprene network since the scattering contrast of polyisoprene is efficiently large at $\phi_{\text{D-toluene}} = 1.00$. Moreover, it should be noted that the upturn of NR0 at low q, which mainly originates from protein aggregates, is larger by 2 orders of magnitude than that of DPNR even though the scattering contrast of protein $(\rho_P - \rho_S)^2$ is smaller than that of polyisoprene $(\rho_I - \rho_S)^2$ at $\phi_{\text{D-toluene}} = 1.00$. It has been reported that the size of the protein aggregate is the largest among the natural impurities in NR, with the compact structure formed by hydrogen bonding.[16,35] We deduce that this characteristic of the large compact aggregates resulted in the strong scattering intensities in the low q region of NR0, which also will be discussed later. As for the scattering profiles of DPNR, the small upturn appeared though DPNR contains no protein. This upturn demonstrates the long-wavelength concentration fluctuation, indicating the existence of localized clusters in solution. This cluster-like structure has also been observed for such systems as graft copolymers and polyelectrolyte solution.[36−38] Each origin of the cluster formation is known to be the specific interaction between polymers and solvents, e.g., hydrophilic/hydrophobic interaction, affinity with solvent molecule, or solubility. As for the polyisoprene/toluene system, Geissler et al. and Horkay et al. observed a similar upturn and clarified that this upturn originates from the dense cluster of undissolved amorphous polymers.[39,40] In the case of DPNR, on the other hand, DPNR includes phospholipids, which are shown to aggregate together by hydrogen bonding and ionic linkages.[41,42] Hence, we deduce that the upturn of DPNR was caused by the cluster-like structures of polyisoprene chains including phospholipid aggregates. With regard to $I(q)$ of DPNR at $\phi_{\text{D-toluene}} = 1.00$, the theoretical curve fitting could be easily performed because it does not include protein and then it behaves as a simple binary system of polyisoprene networks in solvent. In this case, the observed scattering intensity, $I_{\text{obs}}(q)$ can be given by the following equation;[16,20,39,43]

$$I_{\text{obs}}(q) = \frac{I_L(0)}{1 + q^2\xi^2} + \frac{I_{SL}(0)}{(1 + q^2\Xi^2)^2} + I_{\text{inc}} \qquad (4)$$

where ξ and Ξ are the thermal correlation length (or the mesh size of the network) and the characteristic length of the clusters, respectively.[44−46] $I_L(0)$, $I_{SL}(0)$, and I_{inc} are the prefactor of a Lorentz function, a squared-Lorentz function, and the incoherent scattering, respectively.[16,20,39] eq 4 is widely used for the gel system having the static component (second term) from the introduction of cross-linking or the existence of clusters as well as the thermal component (first term). The curve fitting was performed from $q = 0.003$ to 0.2 Å^{-1} using a standard least-squares procedure. The result of curve fitting is shown by the solid line in Figure 2b. The evaluated value of ξ is 15.6 Å and Ξ is 413 Å. The value of ξ is in good agreement with the result of the previous study.[16] It should also be noted that the scattering profiles in the high q regions agreed between NR0 and DPNR, indicating that the size of the partial chains of the polyisoprene network is not influenced by the existence of protein.

3.3. Scattering Intensities of NR0, NR10, and NR20. Figure 3 shows absolute scattering intensities, $I(q)$'s, for NR0, NR10, and NR20 with different $\phi_{\text{D-toluene}}$. The solid lines are reconstructed scattering intensity functions from the obtained partial scattering functions and the estimated scattering length densities, which will be discussed below. The $\phi_{\text{D-toluene}}$ dependence of scattering profiles for NR0, NR10 and NR20 seems to be similar. As discussed above, the large inhomogeneities from protein aggregates are dominating in the low q region, while the network scatterings from polyisoprene chains are the leading terms in the high q regions. $I(q)$'s differed with $\phi_{\text{D-toluene}}$ due to the change of the scattering contrast. That is, with increasing $\phi_{\text{D-toluene}}$, $I(q)$'s once decreased and reached their minimums in the vicinity of $\phi_{\text{D-toluene}} = 0.2$, then increased. Moreover, it should be noted that the profiles of $I(q)$'s in the low q region did not show parallel behaviors and delicately changed with increasing $\phi_{\text{D-toluene}}$, i.e., the slopes of $I(q)$'s at low q get steeper gradually with increasing $\phi_{\text{D-toluene}}$. This indicates that the structures of aggregates consisting of proteins or polyisoprene chains are obviously different and both inhomogeneities in the low q region shown in Figure 2 contribute to the change of $\phi_{\text{D-toluene}}$ dependence of $I(q)$'s.

Let us discuss the scattering intensities in the low q region in more detail. Figure 4 shows $I(q)$'s at $q = 0.004$ Å^{-1}, which can be simply regarded as low q limit in the experimental q range, for NR0, NR10 and NR20. As shown in the figure, each result showed clear parabolic shapes shown by the solid curves. Theoretically, the scattering intensity at a certain q value is a parabolic function as a function of $\phi_{\text{D-toluene}}$ (see eqs 1 and 2). Therefore, the experimental fact of the clear parabolic shapes of $I(q)$'s means that the tuning of the scattering contrast was precisely performed. The evaluated total matching points of the system, where $I(q)$'s become

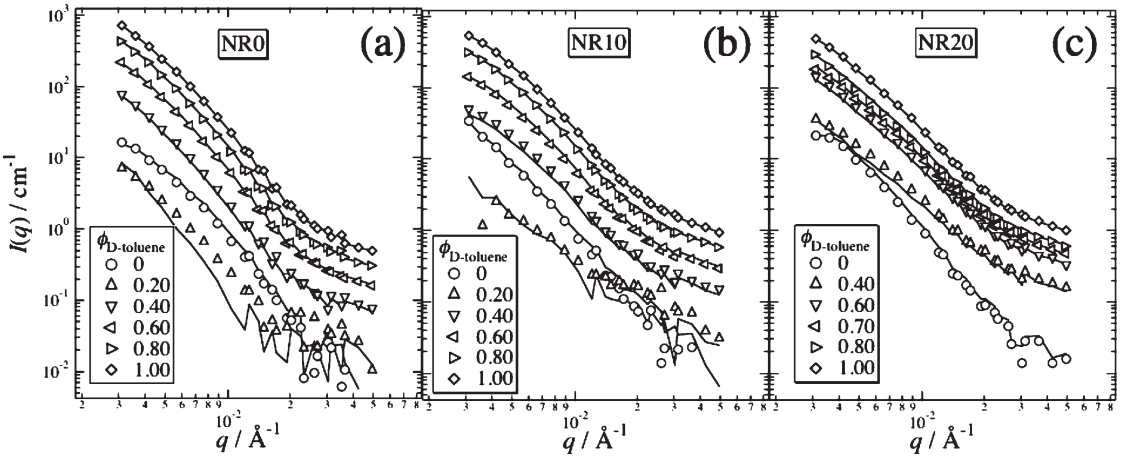

Figure 3. $I(q)$'s for (a) NR0, (b) NR10, and (c) NR20 with different $\phi_{D\text{-toluene}}$. The solid lines are reconstructed scattering intensity functions from obtained partial scattering functions.

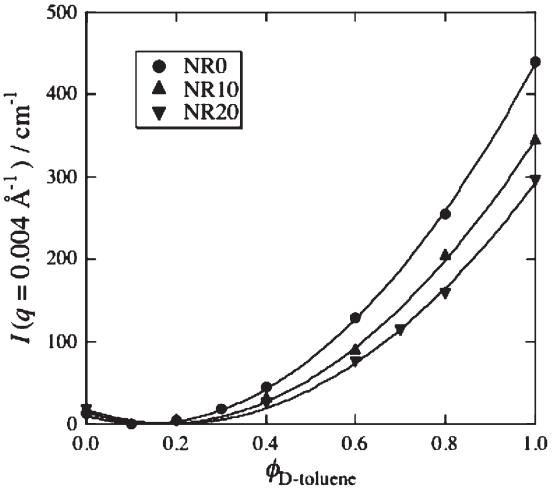

Figure 4. $I(q)$'s at $q = 0.004$ Å^{-1} for NR0, NR10, and NR20. Each solid curve is a fitting curve with a parabolic function.

minimum, were determined to be around $\phi_{D\text{-toluene}} = 0.1-0.2$, irrespective of the degree of cross-linking. This proves the scattering from the protein is sufficiently dominant because the evaluated matching points are located around that of the protein. Moreover, it should be noted that $I(q)$'s at the lowest q ($= 0.004$ Å^{-1}) decreased with the increase of DCP content. This seems to be an unexpected result because the inhomogeneities in polymer network generally increase with the introduction and/or the increase of cross-links. Considering the fact that the contribution to the scattering intensities from DCP is negligible, it should be deduced that the microstructures of protein or polyisoprene chains and/or the interaction between them were changed by peroxide cross-linking. Because the volume fraction of DCP is much less than 1 vol % and the scattering from phospholipids can be included into polyisoprene, the natural rubber system can be treated as three-component system. Therefore, the scattering intensities of the systems can be described by eq 1. Consequently, the origin of the decrease of $I(q)$'s with DCP can be investigated by detailed analyses of $S_{PP}(q)$, $S_{II}(q)$, or $S_{PI}(q)$. Next, we shall discuss the structural change of protein and polyisoprene by DCP cross-linking on the basis of the detailed analyses of the obtained partial scattering functions.

3.4. Partial Scattering Functions. In order to obtain the partial scattering functions by means of CV-SANS, the scattering length densities (SLD) for each component should be known as precisely as possible. In this study, SLD of the polyisoprene and toluene could be determined with a high degree of accuracy from their chemical structures and mass densities, while that of the protein, ρ_P, was uncertain, since the specific volumes of amino acids in toluene could not be experimentally investigated as described in section 3.1. Therefore, the dependence of the partial scattering functions on ρ_P was carefully examined.

Figure 5 shows the partial scattering functions for NR0, NR10, and NR20 by applying $\rho_P = 1.8 \times 10^{10}$ cm^{-2}. The reconstructed intensities from the obtained partial scattering functions and the applied SLD of each component are compared with the measured intensities in Figure 3, which nearly correspond to each other. This strongly suggests that the value of ρ_P would be in the vicinity of that in water. We will discuss the obtained $S_{PP}(q)$ and $S_{II}(q)$ quantitatively below since $S_{PP}(q)$ and $S_{II}(q)$ are stable in respect to a slight variation of ρ_P. $S_{PP}(q)$'s are one or 2 orders of magnitude larger than $S_{II}(q)$'s for the all conditions. This confirms that $S_{PP}(q)$ is responsible for the steep upturn in $I(q)$ of NR0 in parts a and b of Figure 2, and $S_{II}(q)$ is for the small upturn in $I(q)$ of DPNR in Figure 2b. It is obvious that $S_{PP}(q)$'s do not depend on DCP contents. Therefore, we can directly conclude that the local structures of protein aggregates did not change by peroxide cross-linking. On the other hand, $S_{II}(q)$ in the low q region clearly decreased with DCP as shown in Figure 5c. This is rather surprising because the scattering intensities in the low q region are generally known to increase by the introduction of cross-linking, indicating the enhancement of static inhomogeneities. We deduce that this paradoxical result derives from the large inhomogeneities of polyisoprene clusters, which already exists even for solution state (NR0). In contrast to inhomogeneization of network, cross-linking has another role, i.e., pinning or fixation of the structure against a change of its environment.[47,48] Therefore, it should be presumable that the inhomogeneous structure of the polyisoprene clusters is prevented from further inhomogenization by immersing in toluene due to the pinning effect of cross-linking. In addition, the decrease in the scattering intensities in the low q region with increasing DCP is also observed in the previous paper by Karino et al., but the origin was not elucidated.[16] Now, it is disclosed that the introduction of the peroxide cross-linking results in decreases of structural inhomogeneities of polyisoprene matrix, while the structures of the proteins are not affected. It is remarked that the fact that this decrease of S_{II}'s with

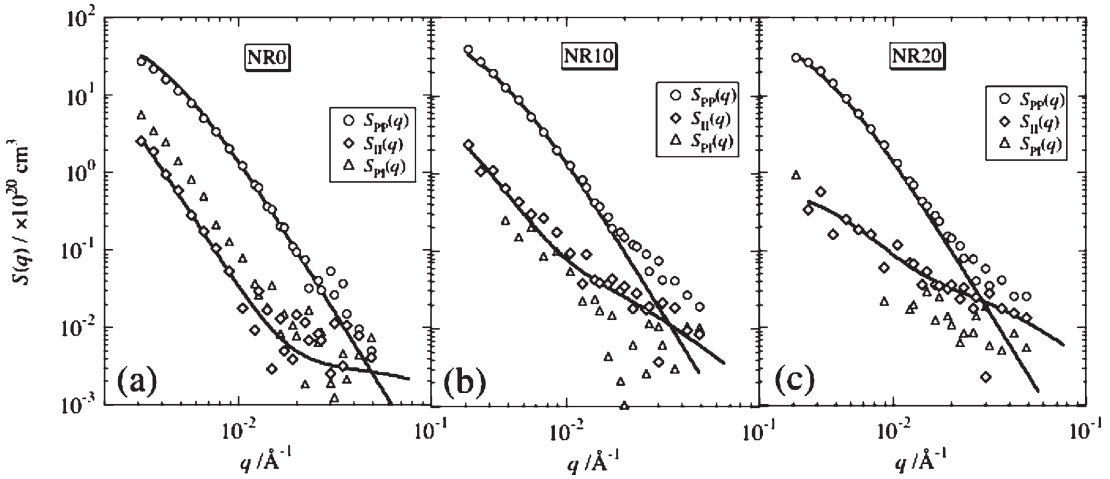

Figure 5. The partial scattering functions for (a) NR0, (b) NR10, and (c) NR20. The solid lines for $S_{PP}(q)$ and $S_{II}(q)$ denote the fits with eqs 5 and 8, respectively. The polymer concentrations were 16.7 vol % for NR0, 17.3 vol % for NR10, and 20.7 vol % for NR20.

DCP was observed by employing the rather wide range of ρ_P, i.e., by considering the error rate of ±10% about ρ_P. In addition, $S_{PI}(q)$ also decreases with increasing DCP mainly due to the change of the local structure of polyisoprene networks.

It was found that the partial scattering functions for proteins, $S_{PP}(q)$, and polyisoprene, $S_{II}(q)$, were rather independent of ρ_P regarding 10% deviation of $\rho_P = 1.8 \times 10^{10}$ cm^{-2} calculated from the specific amount of the proteins in water. On the other hand, the cross term between polyisoprene and protein, $S_{PI}(q)$, was very sensitive to ρ_P. That is, $S_{PI}(q)$ decreases gradually with decreasing of ρ_P, and becomes negative for $\rho_P < 1.7 \times 10^{10}$ cm^{-2}, and increases with increasing of ρ_P. A smaller ρ_P in toluene is due to a lower mass density than that in water. In general, the densities of proteins in toluene would be higher than that in water, since proteins are more or less hydrophilic. Accordingly, the higher density of the protein than that in water would be expected, and positive $S_{PI}(q)$ might be expected in this system. $S_{PI}(q)$ directly reflects the correlation between the polyisoprene and the protein in the system, and the positive sign of $S_{PI}(q)$ indicates that some of polyisoprene chains are anchored by the surface of the protein aggregates.[22,30] The detailed structure of the polyisoprene chains attaching to the surface of the protein aggregates can be explored by $S_{PI}(q)$ in principle. The quantitative discussions about $S_{PI}(q)$, however, should be abandoned due to the uncertainty of ρ_P.

Next, let us discuss the theoretical curve fitting of the partial scattering functions. First, we assume that $S_{PP}(q)$ can be described by a simple spherical function model. In this case, $S_{PP}(q)$ is proportional to both the form factor $P(q)$ and the structure factor $Z(q)$, as described by

$$S_{PP}(q) \propto P(q)Z(q) \tag{5}$$

Here, the form factor $P(q)$ is given by

$$P(q) = \Phi^2(qR_p) \tag{6}$$

$$\Phi(qR_p) = \frac{3[\sin(qR_p) - qR_p\cos(qR_p)]}{(qR_p)^3} \tag{7}$$

where R_p is the radius of the protein aggregates. In order to consider the polydispersity, a Schultz distribution is assumed.[49] On the other hand, the structure factor $Z(q)$ might be unity because the protein concentration is efficiently dilute and hence no interparticle interference is approximated. In addition, taking into account the fact that the obtained $S_{PP}(q)$ agreed with each other irrespective of the DCP contents, we carried out the simultaneous curve fittings to $S_{PP}(q)$'s and obtained $R_p \approx 782$ Å. This value was comparable to the average size of the protein aggregates by AFM observation by Karino et al.[16]

Parts a−c of Figure 5 show that all $S_{II}(q)$'s monotonically decrease from lower-q to higher-q and the slopes at low-q are steeper than those at high-q. Therefore, the intensities were approximated by the phenomenological equation as

$$S_{II}(q) = \frac{S_L(0)}{1+q^2\xi^2} + \frac{S_{SL}(0)}{(1+q^2\Xi^2)^2} \tag{8}$$

Equation 8 consists of a Lorentz function with a prefactor $S_L(0)$ and the size of the density correlation ξ reflecting the intensities at high-q, and a squared-Lorentz function with a prefactor $S_{SL}(0)$ and the characteristic length of inhomogeneities Ξ describing the intensities at low-q, which is the same expression used to describe the small-angle scattering spectra for several gel systems.[16,20,43] In this case, the squared-Lorentz function may include the intensities from several different structural origins. For instance, the contribution of the polyisoprene chains attaching to the protein aggregates is obvious, as the cross term $S_{PI}(q)$ is positive and significantly large as discussed above. In addition, the polyisoprene clusters themselves also can affect the intensities at low-q, which was reported for the randomly cross-linked polyisoprene gels.[50] In case that $S_{PI}(q)$ is quantitatively obtained, it is possible to separate the above structural information.

Figure 6 shows DCP content dependences of (a) ξ and (b) $S_L(0)$. It is rather surprising that ξ increases at the beginning by addition of cross-linker and then decreases. We conjecture that the estimation of the ξ value at DCP = 0 was incorrect and Ξ would be much larger than that at DCP = 1 phr. Because of the strong upturn in $S_{II}(q)$ at low q-region, the Lorentz component in $S_{II}(q)$ is buried in the shoulder of the SL term. If this is the case, it can be concluded that ξ is a decreasing function of cross-linker. The same argument may apply to the discussion of $S_L(0)$. It is clear that the origin of the scattering intensities is the thermal fluctuations in semidilute polyisoprene solutions, and detailed discussion as to the high q region was already given elsewhere.[16]

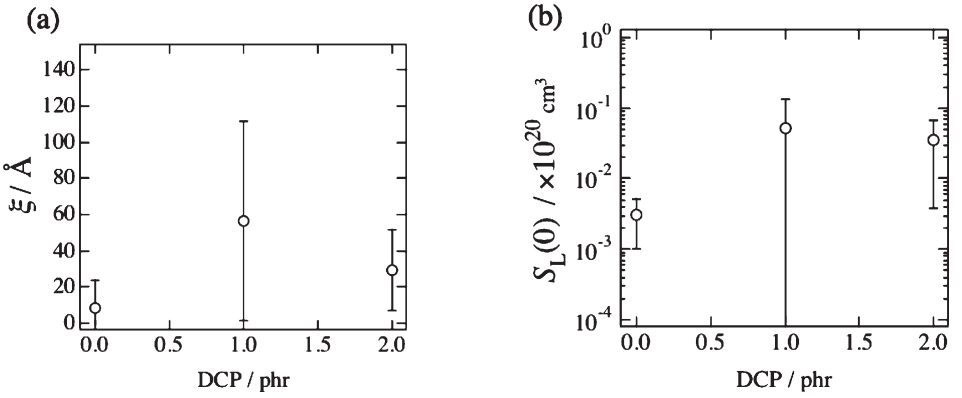

Figure 6. DCP content dependence of (a) the size of the density correlation, ξ, and (b) the prefactor of a Lorentz function, $S_L(0)$.

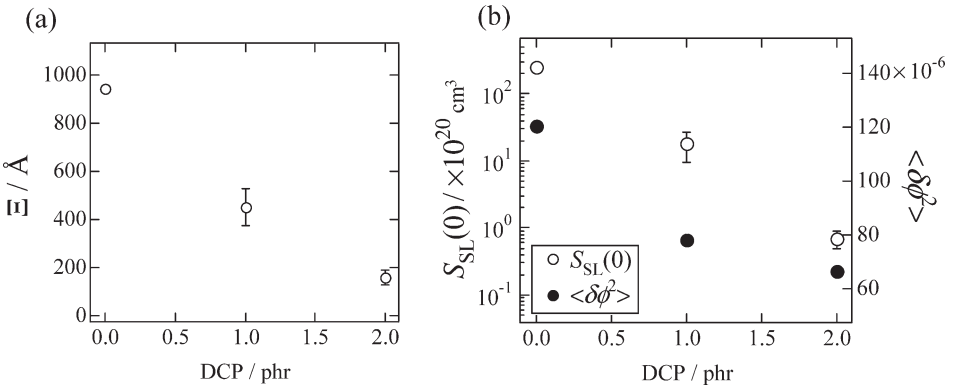

Figure 7. DCP content dependence of (a) the characteristic length of inhomogeneities, Ξ, (b) the prefactor of a squared-Lorentz function, $S_{SL}(0)$, and the mean square amplitude of the static concentration fluctuation, $\langle\delta\phi^2\rangle$.

Figure 7 depicts the DCP content dependences of (a) Ξ and (b) $S_{SL}(0)$ and $\langle\delta\phi^2\rangle$. Here, ϕ is the polymer volume fraction and $\langle\delta\phi^2\rangle$ indicates the mean square amplitude of the static concentration fluctuation, which is given as[43,51]

$$\langle\delta\phi^2\rangle = \frac{S_{SL}(0)}{8\pi\Xi^3} \tag{9}$$

It should be remarkable that not only Ξ but also $S_{SL}(0)$ and $\langle\delta\phi^2\rangle$ decreased with the increase in DCP content. The decrease in Ξ means that large inhomogeneities consisting of the polyisoprene became small and therefore resulted in the rather uniform distribution of the polyisoprene chains by the introduction of DCP cross-linking. Since $S_{SL}(0)$ indicates the intensities scattered by the large inhomogeneities and $\langle\delta\phi^2\rangle$ directly means the static inhomogeneities, the decrease of $S_{SL}(0)$ means that the cluster-like formation rather diminished with the increase in DCP content, being accompanied by the homogeneous network structure. It is clearly proved that the decrease of the total scattering intensities by the addition of DCP exhibited in Figure 4 is due to the structural homogenization of polyisoprene chains in the system at least in this DCP content region.

3.5. Effect of Network Heterogeneity on the Onset of Strain-Induced Crystallization of Peroxide Cross-Linked NR. The observed characteristics on the microscopic structure are useful for understanding the properties of peroxide cross-linked NR: In a previous study by Ikeda et al.,[8,52] for example, the onset strain in the strain-induced crystallization of peroxide cross-linked NR was found to be dependent on its network-chain density, but that of sulfur cross-linked NR was constant regardless of its network-chain density. These observations suggested that the NR networks formed by peroxide and sulfur cross-linking were different, and the network structure of peroxide cross-linked NR was supposed to be more homogeneous when compared with that of sulfur cross-linked NR. However, in this study, the microscopic structure of peroxide cross-linked NR was revealed to be not homogeneous, and it was found to be composed of several kinds of clusters with different sizes, i.e., protein aggregates and polyisoprene clusters. Why did the peroxide cross-linked NR show the strain-induced crystallization behavior like a more homogeneous network than sulfur cross-linked NR? Let us bring the cluster structure (~1000 Å) of polyisoprene in NR0 detected here for considering the phenomenon. The inhomogeneities of polyisoprene are presumable to increase by cross-linking if the introduction of cross-linking simply leads to the enhancement of frozen inhomogeneities. CV-SANS results, on the other hand, clearly suggested that the network becomes less inhomogeneous by introducing cross-linking points as shown in Figure 7. From these results, we estimate that the clustering of polyisoprene was suppressed due to the pinning effect of cross-linking and this fact was revealed by the visualization-by-swelling method. As the result, the overall size of inhomogeneities of peroxide cross-linked NR must have became smaller with an increase of the DCP content, i.e., with a decrease of the inhomogeneities of polyisoprene cluster by cross-linking in the range of this study. Consequently, the mesh size in the matrix that takes a responsibility for causing strain-induced crystallization must have decreased by increasing the cross-linking.[20] In this moment, however, it is not clear why peroxide cross-linking occurs more homogeneously by increasing of cross-linking agent

DCP. The presence of nonrubber components is considered to affect the cross-linking reaction of NR. The detail analysis on the microscopic structures between peroxide cross-linked NR and peroxide cross-linked synthetic isoprene rubber will be reported in a near future. After the investigation, important factors to govern the physical properties of cross-linked NR will be revealed in detail.

4. Concluding Remarks

The microscopic structures of peroxide-cross-linked natural rubber (NR) were investigated by means of contrast-variation small-angle neutron scattering (CV-SANS) as a function of dicumyl peroxide (DCP) content dependence. The existence of the protein aggregates was clearly revealed by SANS, whose structure was hardly affected by the addition of DCP. The scattering function decreased in the low q region with increasing DCP contents. It is disclosed by the obtained partial scattering function, $S_{II}(q)$, that the decrease is originated exclusively from the structural change of the polyisoprene domain or matrix. That is, the inhomogeneities of the polyisoprene chains, or the characteristic size of the clusters, monotonically decreased by the increase of cross-linking. This could be the reason why the onset strain in the strain-induced crystallization of peroxide cross-linked NR is dependent on its network-chain density. This microscopic structural change of polyisoprene networks may play an important role in producing excellent mechanical properties of NR. Further studies on the roles of cross-linking of rubbers are in progress.

Acknowledgment. This work was partially supported by the Ministry of Education, Science, Sports and Culture, Japan (Grantin-Aid for Scientific Research, Nos. 18205025 and 18068004). Japan (Grant-in-Aid for Scientific Research (A), 2006-2008, No. 18205025, and for Scientific Research on Priority Areas, 2006-2010, No. 18068004)). The SANS experiment was performed with the approval of Institute for Solid State Physics, The University of Tokyo (Proposal No. 8604), at Japan Atomic Energy Agency, Tokai, Japan.

References and Notes

(1) Mitchell, G. R. *Polymer* **1984**, *25*, 1562–1572.
(2) Murakami, S.; Senoo, K.; Toki, S.; Kohjiya, S. *Polymer* **2002**, *43*, 2117–2120.
(3) Toki, S.; Sics, I.; Ran, S.; Liu, L.; Hsiao, B. S.; Murakami, S.; Senoo, K.; Kohjiya, S. *Macromolecules* **2002**, *35*, 6578–6584.
(4) Tosaka, M.; Kohjiya, S.; Murakami, S.; Poompradub, S.; Ikeda, Y.; Toki, S.; Sics, I.; Hasiao, B. S. *Rubber Chem. Technol.* **2004**, *77*, 711–723.
(5) Trabelsi, S.; Albouy, P.-A.; Rault, J. *Macromolecules* **2002**, *35*, 10054–10061.
(6) Le Cam, J.-B.; Huneau, B.; Verron, E.; Gornrt, L. *Macromolecules* **2004**, *37*, 5011–5017.
(7) Tosaka, M.; Senoo, K.; Kohjiya, S.; Ikeda, Y. *J. Appl. Phys.* **2007**, *101*, 084909/1–084909/8.
(8) Ikeda, Y.; Yasuda, Y.; Hijikata, K.; Toska, M.; Kohjiya, S. *Macromolecules* **2008**, *41*, 5876–5884.
(9) Bateman, L., *The Chemistry and Physics of Rubber-like Substances*; MacLaren & Sons: London, 1963.
(10) Roberts, A. D., *Natural Rubber Science and Technology*; Oxford Univ. Press: Oxford, U.K., 1988.
(11) Wititsuwannakul, D.; Wititsuwannakul, R. Biochemistry of natural rubber and structure of latex. In *Polyisoprenoids*; Koyama, T., Steinbuchel, A., Eds.; Wiley-VCH: Weinheim, Germany, 2001; Vol. *2*.
(12) Tanaka, Y. *Rubber Chem. Technol.* **2001**, *74*, 355–375.
(13) Yunyongwattanakorn, J.; Sakdapipanich, J. T.; Kawahara, S.; Hirosaka, M.; Tanaka, Y. *J. Appl. Polym. Sci.* **2007**, *106*, 455–461.
(14) Kohjiya, S.; Tosaka, M.; Furutani, M.; Ikeda, Y.; Toki, S.; Hsiao, B. S. *Polymer* **2007**, *48*, 3801–3808.
(15) Kadir, A. A. S. A. *Rubber Chem. Technol.* **1994**, *67*, 537.
(16) Karino, T.; Ikeda, Y.; Kohjiya, S.; Shibayama, M. *Biomacromolecules* **2007**, *8*, 693–699.
(17) Coran, A. Y. *Rubber Chem. Technol.* **1965**, *38*, 1–14.
(18) Coran, A. Y. *J. Appl. Polym. Sci.* **2003**, *87*, 24–30.
(19) Hagen, R.; Salmen, L.; Stenberg, B. *J. Polym. Sci., Part B: Polym. Phys.* **1996**, *34*, 1997–2006.
(20) Ikeda, Y.; Higashitani, N.; Hijikata, K.; Kokubo, Y.; Morita, Y.; Shibayama, M.; Osaka, N.; Suzuki, T.; Endo, H.; Kohjiya, S. *Macromolecules* **2009**, *42*, 2741–2748.
(21) Sirisinha, C.; Phoowakeereewiwat, S.; Saeoui, P. *Eur. Polym. J.* **2004**, *40*, 1779–1785.
(22) Endo, H.; Miyazaki, S.; Haraguchi, K.; Shibayama, M. *Macromolecules* **2008**, *41*, 5406–5411.
(23) Takenaka, M.; Nishitsuji, S.; Amino, N.; Ishikawa, Y.; YAmaguchi, D.; Koizumi, S. *Macromolecules* **2009**, *42*, 308–311.
(24) Okabe, S.; Nagao, M.; Karino, T.; Watanabe, S.; Adachi, T.; Shimizu, H.; Shibayama, M. *J. Appl. Crystallogr.* **2005**, *38*, 1035–1037.
(25) Shibayama, M.; Okabe, S.; Nagao, M.; Sugihara, S.; Aoshima, S.; Harada, T.; Matsuoka, H. *Macromol. Res.* **2002**, *44*, 311.
(26) Shibayama, M.; Nagao, M.; Okabe, S.; Karino, T. *J. Phys. Soc. Jpn.* **2005**, *74*, 2728–2736.
(27) Nieh, M.-P.; Glinka, C. J.; Krueger, S.; Prosser, R. S.; Katsaras, J. *Langmuir* **2001**, *17*, 2629–2638.
(28) Nieh, M.-P.; Glinka, C. J.; Krueger, S.; Prosser, R. S.; Katsaras, J. *Biophys. J.* **2002**, *82*, 2487–2498.
(29) Bacon, G. E. *Neutron Diffraction*; Clarendon: Oxford, U.K., 1975; Vol. *1*.
(30) Miyazaki, S.; Endo, H.; Karino, T.; Haraguchi, K.; Shibayama, M. *Macromolecules* **2007**, *40*, 4287–4295.
(31) Endo, H.; Schwahn, D.; Cölfen, J. *J. Chem. Phys.* **2004**, *120*, 9410–9423.
(32) Jacrot, B. *Rep. Prog. Phys.* **1976**, *39*, 911–953.
(33) Hickl, P.; Ballauff, M. *Physica A* **1997**, *235*, 238–247.
(34) Svergun, D. I.; Koch, M. H. J. *Rep. Prog. Phys.* **2003**, *66*, 1735–1782.
(35) Toki, S.; Burger, C.; Hsiao, B. S.; Amnuaypornsri, S.; Sakdapipanich, J.; Tanaka, Y. *J. Polym. Sci., Part B* **2008**, *46*, 2456.
(36) Hourdet, D.; L'alloret, F.; Durand, A.; Lafuma, F.; Audebert, R.; Cotton, J.-P. *Macromolecules* **1998**, *31*, 5323.
(37) Matsuoka, H.; Schwahn, D.; Ita, N. *Macromolecules* **1991**, *24*, 4227−4228.
(38) Borsali, R.; Nguyen, H.; Pecora, R. *Macromolecules* **1998**, *31*, 1548−1555.
(39) Horkay, F.; Basser, P. J.; Hecht, A. M.; Geissler, E. *Macromolecules* **2000**, *33*, 8329–8333.
(40) Geissler1, E.; Horkay, F.; Hecht1, A.-M.; Deschamps, P.; d'Heres, S. M. *KGK Kautschuk Gummi Kunstst.* **2001**; p 446.
(41) Tarachiwin, L.; Sakdapipanich, J.; Ute, K.; Kitayama, T.; Bamba, T.; Fukusaki, E.; Kobayashi, A.; Tanaka, Y. *Biomacromolecules* **2005**, *6*, 1851–1857.
(42) Tarachiwin, L.; Sakdapipanich, J.; Ute, K.; Kitayama, T.; Tanaka, Y. *Biomacromolecules* **2005**, *6*, 1858–1863.
(43) Geissler, E.; Horkay, F.; Hecht, A. M.; Rochas, C.; Lindner, P.; Bourgaux, C.; Couarraze, G. *Polymer* **1997**, *38*, 15.
(44) Shibayama, M. *Macromol. Chem. Phys.* **1998**, *199*, 1–30.
(45) Shibayama, M.; Isono, K.; Okabe, S.; Karino, T.; Nagao, M. *Macromolecules* **2004**, *37*, 2909–2918.
(46) de Gennes, P. G., *Scaling Concepts in Polymer Physics*. Cornell University: Ithaca, NY, 1979.
(47) Ikkai, F.; Shibayama, M. *J. Polym. Sci., Part B, Polym. Phys. Ed.* **2005**, *43*, 617–628.
(48) Nasimova, I. R.; Karino, T.; Okabe, S.; Nagao, M.; Shibayama, M. *Macromolecules* **2004**, *37*, 8721–8729.
(49) Bartlett, P.; Ottewill, R. H. *J. Chem. Phys.* **1992**, *96*, 3306.
(50) Horkay, F.; McKenna, G. B.; Deschamps, P.; Geissler, E. *Macromolecules* **2000**, *33*, 5215–5220.
(51) Horkay, F.; Hecht, A. M.; Mallam, S.; Geissler, E.; Rennie, A. R. *Macromolecules* **1991**, *24*, 2896.
(52) Ikeda, Y.; Yasuda, Y.; Makino, S.; Yamamoto, S.; Tosaka, M.; Senoo, K.; Kohjiya, S. *Polymer* **2007**, *48*, 1171–1175.